Theory of Distributed Mixing and Amplification in a Superconducting Quasi-Particle Nonlinear Transmission Line

Cheuk-yu Edward Tong, *Member, IEEE*, Linda Chen, and Raymond Blundell, *Member, IEEE*

***Abstract*— An analysis is presented for the behavior of the superconducting quasi-particle nonlinear transmission line driven by a high-frequency local oscillator (LO). The theory developed includes a large-signal nonlinear analysis, a small-signal analysis, and a noise analysis. This model is used to simulate the conversion loss and noise temperature of distributed quasi-particle mixers based on the nonlinear transmission line. The numerical results are compared to an experimental mixer at 460 GHz. The theory also predicts that the nonlinear transmission line will provide parametric amplification when the idler frequency is inductively tuned. This new phenomenon may present new opportunities to low-noise receiver systems at submillimeter wavelengths.**

***Index Terms*—Distributed mixers, nonlinear transmission lines, parametric amplifier, SIS mixers, submillimeter waves.**

I. Introduction

THE distributed mixer based on the nonlinear quasi-particle tunnel current in a superconductor–insulator–superconductor (SIS) nonlinear transmission line has emerged as a new class of low-noise frequency mixers for submillimeter waves [1], [2]. Compared to the conventional lumped-element SIS mixer, the traveling-wave mixer requires a lower critical current-density tunnel barrier, simpler matching circuitry, and lower magnetic field to operate. Therefore, the design and modeling of quasi-particle nonlinear transmission lines are important to submillimeter receiver technology.

The quantum theory of mixing introduced by Tucker [3] provides a solid framework for understanding the behavior of the lumped-element SIS mixer. In order to cover the phenomenon of distributed mixing, this theory has to be extended. Using a three-frequency approximation, in which the effects of harmonic currents are neglected, a numerical model for the frequency-mixing process in an SIS nonlinear transmission line has been developed. The analytical procedure involves three steps. First, the voltage and current waveforms along the line driven by the incident local oscillator (LO) power are solved in the large-signal nonlinear analysis. Then, the linear relationships between the sideband voltages and currents along the line are developed in a linear small-signal analysis, from which the conversion efficiencies between different sidebands can be derived. The third step is a noise analysis in which the sensitivity, or the noise temperature of the mixer, is calculated by summing the shot noise contributions from the entire line. In this paper, the details of the three-step formulation and the results of the authors' numerical simulation are presented.

Manuscript received October 10, 1996; revised March 24, 1997.

C. E. Tong and R. Blundell are with the Harvard–Smithsonian Center for Astrophysics, Cambridge, MA 02138 USA.

L. Chen is with the Department of Mathematics, University of Chicago, Chicago, IL 60615 USA.

Publisher Item Identifier S 0018-9480(97)04459-1.

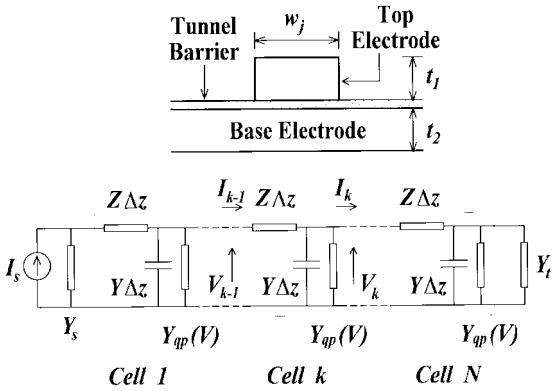

Fig. 1. (Top) Cross-sectional view of a superconducting quasi-particle nonlinear transmission line. (Bottom) Equivalent circuit used in the large-signal analysis of the nonlinear problem.

Although this model has been developed in the context of the SIS distributed mixer, the algorithms implemented can also be adapted to model distributed mixing and frequency multiplication in normal-conducting nonlinear transmission lines. In particular, this numerical model predicts that parametric amplification is feasible in a quasi-particle nonlinear transmission line. Thus, a section of this paper is dedicated to the study of this potential new application of distributed amplification at submillimeter wavelengths.

II. Large-Signal Analysis

A. Equivalent Circuit

Fig. 1(top) shows the cross-sectional view of a superconducting nonlinear transmission line. It is basically a microstrip line with a very thin dielectric insulator, which forms the tunnel barrier for the junction. In this numerical model, the transmission line of length L_j is decomposed into N sections, each of length Δz, as shown in Fig. 1(bottom). Following standard transmission-line theory, each cell contains a series impedance $Z\Delta z$ and a shunt admittance $Y\Delta z$. The nonlinear quasi-particle tunneling current is modeled as a voltage-controlled shunt admittance $Y_{qp}(V)$. The per-unit-

length admittance Y is dictated by the geometrical capacitance of the device itself while the per-unit-length series impedance Z is dominated by the kinetic inductance of the superconducting electrodes [4]

$$Y(\omega) = j\omega w_j C_j \tag{1}$$

$$Z(\omega) = j\frac{\omega\mu_0\lambda_L}{w_j}\left[\coth\left(\frac{t_1}{\lambda_L}\right) + \coth\left(\frac{t_2}{\lambda_L}\right)\right] \tag{2}$$

where C_j is the specific capacitance (per unit area) of the SIS junction, λ_L is the penetration depth, w_j is the width of the line, and t_1 and t_2 are the thicknesses of the electrodes. Note that (2) is formulated with the two-fluid model and is valid at frequencies well below the band-gap frequency of the superconductor ($\nu_g \sim 700$ GHz for niobium).

The nonlinear quasi-particle shunt admittance $Y_{qp}(V)$ is readily derived from Tucker's theory [3]

$$Y_{qp}(V) = \frac{1}{|V|}\left\{\sum_{n=-\infty}^{\infty} J_n(\alpha)[J_{n-1}(\alpha) + J_{n+1}(\alpha)]I_{dc}\left(V_b + \frac{n\hbar\omega}{e}\right) + j\sum_{n=-\infty}^{\infty} J_n(\alpha)[J_{n-1}(\alpha) - J_{n+1}(\alpha)]I_{kk}\left(V_b + \frac{n\hbar\omega}{e}\right)\right\} \tag{3}$$

where $\alpha = e|V|/\hbar\omega$ is the normalized LO drive voltage, V_b is the dc bias voltage, $I_{\rm dc}$ is the dc-current–voltage characteristic of the cell, and $I_{\rm kk}$ is its Kramers–Kronig transform. Since there are a total of N cells, $I_{\rm dc}$ is N times smaller than the measured value for the entire device.

Using this equivalent circuit, the large-signal problem reduces to a search for the set of output voltage and current of each cell V_k and I_k, which satisfy the boundary conditions imposed by the large-signal LO drive I_s, the embedding admittance Y_s, and the terminating admittance Y_t to the line.

B. Linear Approximation

As in most numerical methods, the numerical solution of the above equivalent circuit requires an initial trial solution. A linear approximation of the nonlinear problem turns out to be a good starting point.

In this approach, the nonlinear tunneling admittance is replaced by a constant conductance distributed uniformly along the nonlinear transmission line. Thus, Y_{qp} is replaced by $G\Delta z$ in each of the N cells. A convenient choice of the total distributed conductance GL_j is the optimal source conductance of a nondistributed SIS mixer using a lumped-element junction with a normal-state conductance G_N, identical to the authors' long junction [5]. In the authors' simulation, the per-unit-length conductance employed is

$$G = \frac{G_N}{L_j}\left(0.28 + \frac{0.4\nu_g}{\nu}\right). \tag{4}$$

The resulting linear network can be solved analytically with standard transmission line theory as follows:

$$Y_c V(z) = I^+\exp(-\gamma z)\{1 + \Gamma(Y_t)\exp[2\gamma(z - L_j)]\} \tag{5}$$

$$I(z) = I^+\exp(-\gamma z)\{1 - \Gamma(Y_t)\exp[2\gamma(z - L_j)]\} \tag{6}$$

where

$$I^+ = \frac{Y_c I_s}{Y_c + Y_s}[1 - \Gamma(Y_s)\Gamma(Y_t)\exp(-2\gamma L_j)]^{-1} \tag{7}$$

$$Y_c = \sqrt{(Y + G)/Z} \tag{8}$$

$$\gamma = \sqrt{Z(Y + G)} \tag{9}$$

$$\Gamma(Y) = (Y_c - Y)/(Y_c + Y). \tag{10}$$

Y_c is the characteristic admittance of the linearized transmission line and γ is its propagation constant. The source and termination are located at $z = 0$ and L_j, respectively.

C. Formulation

Classical mixer theory uses a voltage-update method to solve the nonlinear large-signal problem [6]. A similar approach is used here. Since the voltage and current waveforms along a transmission line form a pair of coupled differential equations, it is necessary to simultaneously integrate both of them in the formalism. Therefore, the $ABCD$ matrix approach has been selected to analyze the equivalent circuit of Fig. 1(b).

The input voltage and current of the cell k, V_{k-1}, and I_{k-1} are related to the output voltage and current V_k and I_k through the matrix relation

$$\begin{pmatrix} V_{k-1} \\ I_{k-1} \end{pmatrix} = \begin{pmatrix} A_k & B_k \\ C_k & D_k \end{pmatrix}\cdot\begin{pmatrix} V_k \\ I_k \end{pmatrix} = \begin{pmatrix} 1 & Z\Delta z \\ Y_k & 1 + Y_k Z\Delta z \end{pmatrix}\cdot\begin{pmatrix} V_k \\ I_k \end{pmatrix} \tag{11}$$

where

$$Y_k = Y_{qp}(V_k) + Y\Delta z. \tag{12}$$

The cascaded $ABCD$ matrix of the entire transmission line is

$$\begin{pmatrix} A_l & B_l \\ C_l & D_l \end{pmatrix} = \prod_{k=1}^{N}\begin{pmatrix} A_k & B_k \\ C_k & D_k \end{pmatrix}. \tag{13}$$

The input admittance of the line terminated by an admittance Y_t is

$$Y_{\rm in} = \frac{C_l + D_l Y_t}{A_l + B_l Y_t} \tag{14}$$

from which the input voltage and current to the first cell can be derived as follows:

$$I_0 = I_s Y_{\rm in}/(Y_{\rm in} + Y_s) \tag{15}$$

$$V_0 = I_0/Y_s. \tag{16}$$

Once V_0 and I_0 are known, a new set of voltages and currents $(V_k\ I_k)^T$ can be obtained by using the recurrence relation (11).

Therefore, starting with an initial trial solution set $V_k = V(k\Delta z)\quad (k = 0, \cdots, N)$ given by the linear approximation, the above expressions are applied iteratively to update the solution set. Convergence is considered to be reached if the differences between the amplitudes of all corresponding voltage phasors V_k at two successive iterations are less than 0.1% and the differences between their phases are less than 0.01 rad.

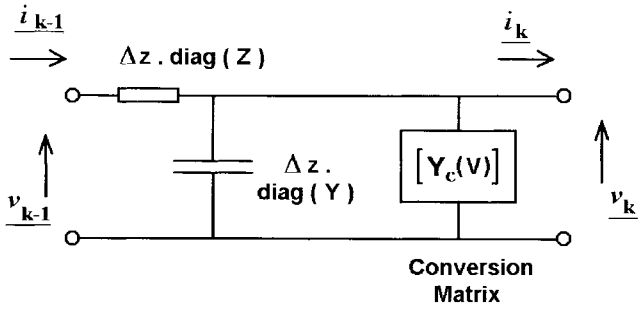

Fig. 2. Equivalent circuit of the cell k in the small-signal analysis. The voltages and currents are denoted as vectors because three different sideband frequencies are involved.

III. Small-Signal Analysis

Tucker has derived the linear relationships between the small-signal sideband voltages and currents for a lumped-element SIS mixer [3]. These equations are conveniently cast into a matrix representation, relating the column vector of sideband currents $\underline{i}$ with the column vector of sideband voltage $\underline{v}$ as follows:

$$\underline{i} = \begin{pmatrix} i_1 \\ i_0 \\ i_{-1} \end{pmatrix} = \mathbf{Y_c}(V) \cdot \begin{pmatrix} v_1 \\ v_0 \\ v_{-1} \end{pmatrix} = \mathbf{Y_c}(V) \cdot \underline{v}. \tag{17}$$

$\mathbf{Y_c}(V)$ is commonly known as the conversion matrix. The elements of $\mathbf{Y_c}$ are functions of the large-signal waveform $V(z)$. The subscripts to the small-signal voltages and currents identify the sideband. Thus i_n is the small-signal current at sideband n, the frequency of which is

$$\omega_n = n\omega_{\mathrm{LO}} + \omega_{\mathrm{IF}}. \tag{18}$$

Only the upper sideband, the IF, and the lower sideband, corresponding to $n = 1, 0$, and -1, respectively, are considered in a three-frequency approximation.

In a lumped-element mixer, the phase of the LO drive does not affect the conversion matrix because one can always arbitrarily set the phase of the LO drive as the reference zero phase. This is not possible in a nonlinear transmission line, as each cell in the line sees a different LO phase. As pointed out in [7], the arguments of nondiagonal elements $\mathbf{Y}_{\mathbf{c}_{m,n}}\,(m \neq n)$ have to be modified as follows:

$$\mathbf{Y}_{\mathbf{c}_{m,n}}(\phi_{\mathrm{LO}}) = \mathbf{Y}_{\mathbf{c}_{m,n}}(\phi_{\mathrm{LO}} = 0) \cdot \exp[j(m-n)\phi_{\mathrm{LO}}] \tag{19}$$

where ϕ_{LO} is the phase of the large-signal LO drive at the cell.

Let $\underline{i}_k$ and $\underline{v}_k$ be the column vectors of sideband currents and voltages at the output of the cell k. Referring to Fig. 2, the following matrix relations can be established:

$$\underline{i}_{k-1} = \underline{i}_k + \Delta z \cdot \mathbf{diag}(Y) \cdot \underline{v}_k + \mathbf{Y_c}(V_k) \cdot \underline{v}_k \tag{20}$$

$$\underline{v}_{k-1} = \underline{v}_k + \Delta z \cdot \mathbf{diag}(Z) \cdot \underline{i}_{k-1} \tag{21}$$

where

$$\mathbf{diag}(X) = \begin{pmatrix} X(\omega_1) & 0 & 0 \\ 0 & X(\omega_0) & 0 \\ 0 & 0 & X(\omega_{-1}) \end{pmatrix}. \tag{22}$$

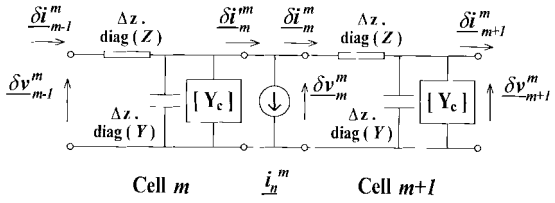

Fig. 3. Equivalent circuit of noise analysis showing cells m and $m+1$. Here, the noise contribution due to the tunneling current in cell m is considered. This source of shot noise is represented by an equivalent noise-current source placed at the output of the cell.

Note that the impedances and admittances involved in the small-signal analysis may be different for the different sidebands and are, therefore, expressed as a function of frequency. The boundary condition at the termination of the line is

$$\underline{i}_N = \mathbf{diag}(Y_t) \cdot \underline{v}_N. \tag{23}$$

Starting from this equation, the recurrence relations (20) and (21) can be used to construct the matrixes $\mathbf{S}$ and $\mathbf{T}$, which relate the input current and voltage vectors with the voltage vector at the following termination:

$$\underline{i}_0 = \mathbf{S} \cdot \underline{v}_N \tag{24}$$

$$\underline{v}_0 = \mathbf{T} \cdot \underline{v}_N. \tag{25}$$

Let $\underline{i_s}$ be the small-signal current source driving the line. Thus

$$\underline{i_s} = \underline{i}_0 + \mathbf{diag}(Y_s) \cdot \underline{v}_0 = \{\mathbf{S} \cdot \mathbf{T}^{-1} + \mathbf{diag}(Y_s)\} \cdot \underline{v}_0. \tag{26}$$

Note that the matrix $\{\mathbf{S} \cdot \mathbf{T}^{-1} + \mathbf{diag}(Y_s)\}$ corresponds to the augmented $\mathbf{Y}'$ matrix in the standard lumped-element mixer theory [6]. At this point, one can just follow the standard approach in the mixer analysis and write

$$\mathbf{Z}' = \{\mathbf{S} \cdot \mathbf{T}^{-1} + \mathbf{diag}(Y_s)\}^{-1}. \tag{27}$$

In a distributed mixer, the IF output can be obtained from either end of the transmission line. Here, the IF termination is assumed to be at the input side. The single-sideband (SSB) conversion gain of the mixer can be written as

$$G_{\mathrm{SSB}} = 4\mathrm{Re}\,(Y_s(\omega_1))\mathrm{Re}(Y_s(\omega_0))|\mathbf{Z}'_{01}|^2. \tag{28}$$

IV. Noise Analysis

The basic assumption of the noise analysis is that the shot noise created by bursts of tunneling current at any point along the nonlinear transmission line is not correlated with the shot noise generated at any other point. Starting from this assumption, one can see that the total noise power delivered to the IF termination is simply the sum of the contributions from each equivalent shot noise-current source associated with each of the cells.

Referring to Fig. 3, the noise contribution from the cell m is now considered. The equivalent shot noise-current source $\underline{i_n}^m$ is placed in a shunt position at the output of the cell. By the theorem of superposition, it is assumed that no other noise-current source is present elsewhere. Let $\underline{\delta i}^m_{k-1}$ and $\underline{\delta v}^m_{k-1}$ be the input noise current and voltage vectors, respectively, at any cell k due to the noise source $\underline{i}^m_n$. The noise current flowing

outwards from cell m toward the noise source $\underline{i}_n^m$ is denoted as $\underline{\delta i'}_m^m$, such that

$$\underline{i}_n^m = \underline{\delta i'}_m^m - \underline{\delta i}_m^m. \tag{29}$$

The recurrence relations (20) and (21) used in the small-signal analysis also apply:

$$\underline{\delta i}_{k-1}^m = \underline{\delta i}_k^m + \Delta z \cdot \mathbf{diag}(Y) \cdot \underline{\delta v}_k^m + \mathbf{Y}_c(V_k) \cdot \underline{\delta v}_k^m \tag{30}$$

$$\underline{\delta v}_{k-1}^m = \underline{\delta v}_k^m + \Delta z \cdot \mathbf{diag}(Z) \cdot \underline{\delta i}_{k-1}^m. \tag{31}$$

It should be noted that in the case of $k = m$, the first term in (30) should be changed to $\underline{\delta i'}_m^m$. The boundary conditions of the above recurrence relations are

$$\underline{\delta i}_0^m = -\mathbf{diag}(Y_s) \cdot \underline{\delta v}_0^m \tag{32}$$

$$\underline{\delta i}_N^m = +\mathbf{diag}(Y_t) \cdot \underline{\delta v}_N^m. \tag{33}$$

Starting from (32) and using the recurrence relations (30) and (31) for $k = 1, 2, \cdots, m$, the matrixes $\mathbf{S}'_m$ and $\mathbf{T}'_m$ are constructed:

$$\underline{\delta i'}_m^m = \mathbf{S}'_m \cdot \underline{\delta v}_0^m \tag{34}$$

$$\underline{\delta v}_m^m = \mathbf{T}'_m \cdot \underline{\delta v}_0^m. \tag{35}$$

Similarly, starting from (33), and using the same recurrence relations for $k = N, (N-1), \cdots, (m+1)$, the matrixes $\mathbf{S}_m$ and $\mathbf{T}_m$ are constructed:

$$\underline{\delta i}_m^m = \mathbf{S}_m \cdot \underline{\delta v}_N^m \tag{36}$$

$$\underline{\delta v}_m^m = \mathbf{T}_m \cdot \underline{\delta v}_N^m. \tag{37}$$

By manipulating (29)–(37), the following matrix equation can be derived:

$$\underline{\delta v}_0^m = \mathbf{Z}^m \cdot \underline{i_n}^m = \left\{\mathbf{S}'_m - \mathbf{S}_m \cdot \mathbf{T}_m^{-1} \cdot \mathbf{T}'_m\right\}^{-1} \cdot \underline{i_n}^m. \tag{38}$$

Following standard noise analysis of lumped-element mixers [6], the mean-square noise voltage at the IF termination due to the noise source $\underline{i}_n^m$ is

$$\left\langle \left| v_n^m \right|^2 \right\rangle = \sum_{k=-1}^{1} \sum_{k'=-1}^{1} \mathbf{Z}_{0k}^m \cdot \left(\mathbf{Z}_{0k'}^m\right)^* \cdot \mathbf{H}_{kk'}^m \tag{39}$$

where $\mathbf{H}^m$ is the current correlation matrix of the cell m [3], [6]. The total noise power delivered to the IF termination is the sum of the contributions from all the cells. Knowing the conversion gain of the mixer, one can establish the SSB noise temperature of the distributed mixer

$$T_{\mathrm{SSB}} = \frac{\mathrm{Re}(Y_s(\omega_0))}{k_B G_{\mathrm{conv}}} \sum_{m=1}^{N} \left\langle \left| v_n^m \right|^2 \right\rangle \tag{40}$$

where k_B is the Boltzmann's constant.

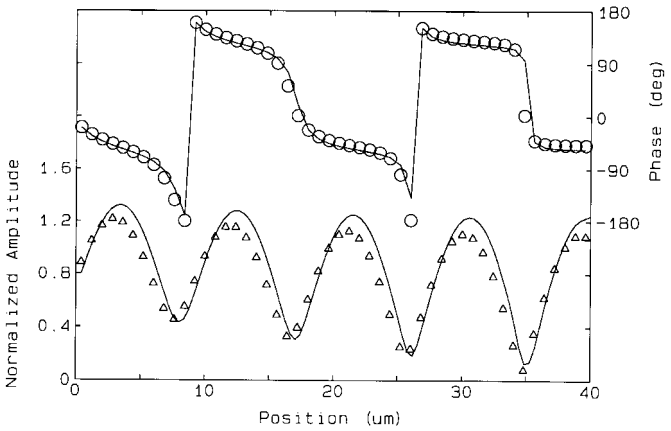

Fig. 4. Large-signal LO voltage waveform along a 150-nm-wide 40-μm-long quasi-particle nonlinear transmission line that has a critical current density of 2.5 kA/cm^2. The LO frequency is 460 GHz and the available LO power is about 135 nW at a source impedance of 8 Ω. The solution of the nonlinear analysis is plotted in $\triangle$ for the normalized RF voltage (in eV/$h\nu$) and $\bigcirc$ for phase. Also shown in solid lines are the amplitude and phase waveform from the linear approximation.

V. Implementation of the Algorithm

In this simulation, the dc characteristic of a generic SIS junction (similar to the one used in [8]) is employed. For niobium junctions, the following material parameters have been employed: $V_g = 2.85$ mV, $\lambda_L = 85$ nm, and $C_j = 65$ fF/μm^2. The mixer under simulation is a double-sideband (DSB) mixer. The embedding admittances at the LO frequency and the upper and lower sidebands are identical and real, such that $Y_s(\omega_{\mathrm{LO}}) = Y_s(\omega_1) = Y_s(\omega_{-1}) = 1/R_s$. The IF termination $1/Y_s(\omega_0)$ is taken to be 50 Ω and the IF is 5 GHz. The nonlinear transmission line is also open at the far end, which is $Y_t(\omega) = 0$.

The algorithm is implemented in C++ running under Windows NT on a Pentium machine. For each set of input data to the program, the LO drive is varied to optimize the SSB conversion gain G_{SSB}. The noise temperature at the optimal LO drive is then computed. Convergence of the nonlinear large-signal problem is readily attained. In fact, including the optimization of LO drive, the central processing unit (CPU) time needed per data set is only about 1 s. The key to this speed of convergence is that the linear approximation given in Section II-B is indeed very close to the nonlinear solution. Fig. 4 shows a comparison between the linear approximation and the nonlinear solution.

The number of cells, N, used in the simulation is usually about 50–80. It has been found that the use of about 15 cells per guided wavelength is generally adequate. For $N > 15L_j/\lambda_g$, the resulting solution is relatively insensitive to N.

VI. Performance of the Distributed SIS Mixer

In order to validate the software, it has been used to simulate the performance of the first 460-GHz distributed mixer designed in the authors' receiver laboratory [1]. In the experimental mixer, a microstrip-transformer section transforms the waveguide circuit impedance to an impedance level of about 8 Ω at the center frequency of 460 GHz. The computer

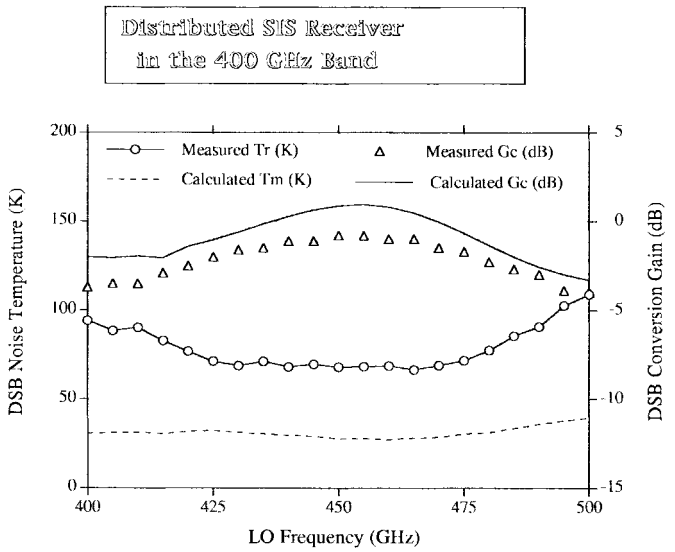

Fig. 5. Comparison between the theoretical and experimental performances of the 460-GHz distributed SIS receiver [1].

model assumes a constant source impedance of 8 Ω across the entire frequency band. The theoretical values are converted into DSB values by multiplying $G_{\rm SSB}$ and dividing $T_{\rm SSB}$ by 2. The parameters of simulation are $J_c = 2.5$ kA/cm^2, $w_j = 150$ nm, $L_j = 40$ μm, $V_b = 2.3$ mV.

Fig. 5 shows the measured DSB conversion loss and receiver noise temperature as well as the computed conversion loss and mixer noise temperature as a function of LO frequency. The measured conversion loss is about 1.5 dB higher than the simulated loss, both centered at about 455 GHz. The model predicts that the 3-dB band edges of the mixer are at 415 and 485 GHz, compared to the measured values of 400 and 500 GHz. Considering the presence of input coupling loss of about 0.5 dB and measurement errors of about ±0.5 dB, it is concluded that the model is in reasonable agreement with the measured data. As for the mixer noise temperature, the experimental value of 18 (±10) K [1] at 460 GHz, compares favorably to the computed value of 27 K. The divergence is roughly that of the quantum noise at this frequency ($h\nu/2k_B \sim 11$ K). The optimum LO drive for the mixer is determined to be of the order of 150 nW for operation across the 400-GHz band, comparable to that of a lumped-element SIS mixer with similar value of R_N [3].

The contour plots of Fig. 6 show how the theoretical SSB conversion gain $G_{\rm SSB}$ and the SSB mixer noise temperature $T_{\rm SSB}$ vary with the source resistance R_s and the length of the device L_j for the same 460-GHz mixer discussed above. The characteristic impedance and guided wavelength at 460 GHz of the nonlinear transmission line are 12 Ω and 18.7 μm, respectively. The plots show that good conversion gains are realizable at low source resistance where the optimum line lengths are spaced $\lambda_g/2$ apart. Local maxima of the mixer noise temperature are also observed at the same values of L_j, but the optimal source resistance is about 8 Ω. The authors' computer model confirms that both the length of the nonlinear transmission line (40 μm) and the source resistance (8 Ω) are well chosen for their experimental receiver.

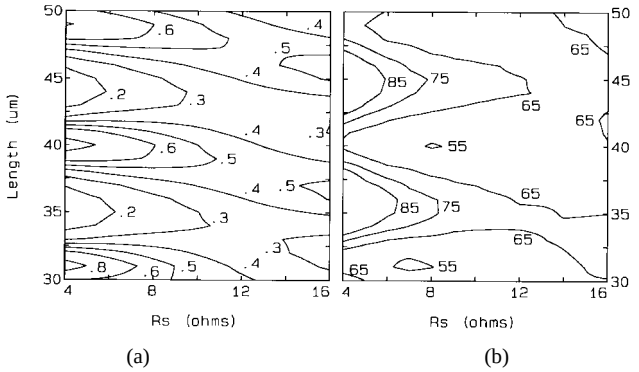

Fig. 6. (a) Theoretical SSB conversion gain contours and (b) theoretical SSB mixer noise temperature (K) contours of a 460-GHz SIS distributed mixer as a function of the source resistance and the length of the nonlinear transmission line.

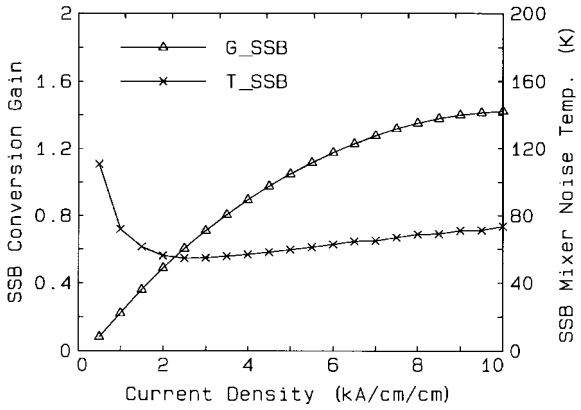

Fig. 7. Dependence of SSB conversion gain and SSB mixer noise temperature on the critical current density of the 460-GHz distributed mixer. The source resistance is kept at 8 Ωand the line length is 40 μm.

The authors' simulation suggests that both the conversion efficiency and mixer noise temperature will generally improve when L_j is reduced. This is consistent with the fact that at longer line lengths, the IF output capacitance is higher and that the far end of the line contributes more noise, but little to conversion efficiency. The minimum $T_{\rm SSB}$ of about 55 K given in the figure corresponds to about 2.5 $h\nu/k_B$. This is higher than the theoretical minimum noise temperature of lumped-element SIS mixers which can be as low as $h\nu/2k_B$. Lower noise temperature may be obtained by reducing L_j, but at the expense of higher critical current density of the tunnel barrier.

In Fig. 7, $G_{\rm SSB}$ and $T_{\rm SSB}$ are plotted as a function of J_c for $R_s = 8\,\Omega$ and $L_j = 40$ μm at 460 GHz. Minimum mixer noise temperature occurs at $J_c = 2.5$ kA/cm^2, but the conversion efficiency increases with J_c. In [2], a design rule of

$$GZ_c > 1.4 \tag{41}$$

was proposed from empirical considerations. Using (4) and the relation between J_c and G_N for niobium junctions

$$J_c w_j L_j = 0.0019 G_N \tag{42}$$

the design rule of (41) implies that for the nonlinear transmission line under consideration $J_c > 3.7$ kA/cm^2. Fig. 7 shows that at this value of critical current density, the mixer conversion gain is about unity, and the noise temperature is

close to its minimum value realized at $J_c \sim 2.5$ kA/cm^2. Therefore, for most ultrahigh sensitive SIS receiver systems, the rule $GZ_c \sim 1.4$ represents a reasonable tradeoff.

VII. Parametric Amplification

In the simulation of the phenomenon of distributed mixing in a quasi-particle nonlinear transmission line, the line used is open at the far end. It is found that when an RF load is introduced at the end of the line while maintaining $Y_t(\omega_0) = 0$, the signal waveform along the line may be amplified parametrically if $Y_s(\omega_0)$ is purely inductive. In this way, more signal power is delivered to the RF load than is fed into the line from the source in the presence of the large-signal LO drive. It is well known that lumped-element SIS mixers can exhibit signal reflection gain [9]. However, such a situation is usually not useful because the input impedance of the mixer may be negative and a circulator is needed to exploit the potential amplification. However, in a nonlinear transmission-line parametric amplifier, no circulator is required and the input impedance is not usually negative.

The formulation developed in the Sections II–IV also applies to the traveling-wave parametric amplifiers. The gain of the amplifier $G_{\rm para}$ and its noise temperature $T_{\rm amp}$ may be derived as follows:

$$G_{\rm para} = 4{\rm Re}(Y_s(\omega_1)){\rm Re}(Y_t(\omega_1))|\mathbf{Z}''_{11}|^2 \tag{43}$$

$$T_{\rm amp} = \frac{{\rm Re}(Y_t(\omega_1))}{k_B G_{\rm para}} \sum_{m=1}^{N} \sum_{k=-1}^{1} \sum_{k'=-1}^{1} \mathbf{Z}^m_{\mathbf{a}_{1k}} \cdot \left(\mathbf{Z}^m_{\mathbf{a}_{1k'}}\right)^* \cdot \mathbf{H}^m_{kk'} \tag{44}$$

where

$$\mathbf{Z}'' = \mathbf{T}^{-1} \cdot \mathbf{Z}' \tag{45}$$

$$\mathbf{Z}^m_{\mathbf{a}} = \left\{\mathbf{S}'_m \cdot \mathbf{T}'^{-1}_m \cdot \mathbf{T}_m - \mathbf{S}_m\right\}^{-1}. \tag{46}$$

In a parametric amplifier, the sideband 0 at ω_0 is commonly referred to as the idler. The large-signal drive is referred to as the pump. The authors' have investigated the use of the same nonlinear transmission line simulated in the above section as a parametric amplifier. The pump frequency is set to be 460 GHz and the idler is set to be 5 GHz. The source and terminating impedances of the transmission line in the 400-GHz band are taken to be 8 μm. The line is open at the far end at the idler frequency, which is $Y_t(\omega_0) = 0$. The resulting signal gain at 465 GHz and the expected amplifier noise temperature are presented as contour plots in Fig. 8 as a function of the reactive idler load $X_i = 1/Y_s(\omega_0)$ and the length of the line.

Fig. 8 shows that a peak gain of about 5.2 can be obtained with $X_i = 27\ \Omega$ and $L_j = 99\ \mu$m, or about 5.4 λ_g. At this point, the required pumping power is about 300 nW and the input return loss is about -16 dB. Local gain maxima are also observed at $L_j = 90\ \mu$m, $X_i = 30\ \Omega$, where the gain is about 5.0 and again at $L_j = 81\ \mu$m, $X_i = 33\ \Omega$, where the gain is about 4.7. As in the distributed mixer, the optimum line length repeats every $\lambda_g/2$. The optimum value of X_i at the local gain maxima is found to be around $0.8/(\omega_0 w_j L_j C_j)$. In other words, at the idler frequency, the inductive load should roughly tune out the capacitance of the entire line.

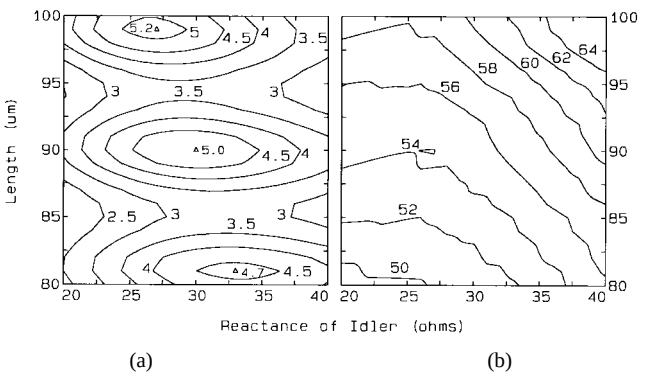

(a) (b)

Fig. 8. (a) Theoretical gain contours and (b) theoretical amplifier noise temperature (K) contours of a quasi-particle nonlinear transmission-line parametric amplifier as a function of the reactive load at the idler frequency and the length of the nonlinear transmission line. The frequency of the parametric pump is 460 GHz.

The noise temperature generally increases with L_j and X_i over our simulated range. Therefore, the optimum line length should be trading off gain and noise temperature. In any case, the simulated noise temperature of the parametric amplifier is comparable to that of the distributed mixer.

Up until now, only a small part of the parameter space has been explored. However, the authors' model does predict low-noise stable gain from this new class of parametric amplifier. This would certainly open up the horizon of exciting new applications in the submillimeter spectrum.

VIII. Conclusion

A complete theory including nonlinear, small-signal, and noise analysis has been developed for characterizing quasi-particle nonlinear transmission lines. This theory has been applied to model distributed SIS mixers. The numerical results have been compared to experimental data. Using the authors' computer model, it has been discovered that the nonlinear transmission line can be used as a parametric amplifier when the idler frequency is inductively terminated. This new phenomenon of parametric amplification can open new possibilities in the submillimeter spectrum.

Acknowledgment

The authors would like to thank Dr. M. Feldman of the University of Rochester for his valuable discussions.

References

[1] C. E. Tong, R. Blundell, B. Bumble, J. A. Stern, and H. G. LeDuc, "Quantum limited heterodyne detection in superconducting nonlinear transmission lines at sub-millimeter wavelengths," *Appl. Phys. Lett.*, vol. 67, pp. 1304–1306, Aug. 1995.

[2] ——, "Distributed quasi-particle mixing in nonlinear transmission lines at sub-millimeter wavelengths," presented at the *Appl. Superconductivity Conf.*, Pittsburgh, PA, paper ET-8, Aug. 1996.

[3] J. R. Tucker and M. J. Feldman, "Quantum detection at millimeter wavelengths," *Rev. Mod. Phys.*, vol. 57, pp. 1055–1113, 1985.

[4] T. Van Duzer and C. W. Turner, *Principles of Superconductive Devices and Circuits.* New York: Elsevier, 1980.

[5] Q. Ke and M. Feldman, "Optimum source conductance for high-frequency superconducting quasi-particle receivers," *IEEE Trans. Microwave Theory Tech.*, vol. 41, pp. 600–604, 1993.

[6] D. H. Held and A. R. Kerr, "Conversion loss and noise of microwave and millimeter-wave mixers: Part I—Theory," *IEEE Trans. Microwave Theory Tech.*, vol. MTT-26, pp. 49–55, 1978.
[7] J. Zmuidzinas, H. G. LeDuc, J. A. Stern, and S. R. Cypher, "Two-junction tunning circuits for submillimeter SIS mixers," *IEEE Trans. Microwave Theory Tech.*, vol. 42, pp. 698–706, 1994.
[8] C. E. Tong and R. Blundell, "Simulation of the superconducting quasi-particle mixer using a five-port model," *IEEE Trans. Microwave Theory Tech.*, vol. 38, pp. 1391–1398, Oct. 1990.
[9] M. J. Feldman, "Some analytical and intuitive results in the quantum theory of mixing," *J. Appl. Phys.*, vol. 53, pp. 584–592, 1982.

Cheuk-yu Edward Tong (M'89) was born in Hong Kong. He received the B.Sc. (Eng.) degree from the University of Hong Kong in 1983, and the Diplôme d'Ingénieur degree from the engineering school ENSERG in Grenoble, France, in 1985.

From 1985 to 1988, he was with the Institut de Radio Astronomie Millimétrique in Grenoble, France, where he studied low-noise superconducting receivers for millimeter wavelengths. In 1988, he received the Ph.D. degree from the Université de Joseph Fourier, Grenoble, France. From 1989 to 1991, he was a Post-Doctoral Fellow at the Communications Research Laboratory, Tokyo, Japan. Since 1991, he has been with the Harvard–Smithsonian Center for Astrophysics, Cambridge, MA, where he is a staff member responsible for the development of ultra-sensitive superconducting receivers for submillimeter waves. He is also an Astronomy Lecturer, Harvard University, Cambridge, MA. His research interests include superconducting devices and their applications to high frequencies, low-noise heterodyne instrumentation, submillimeter and quasi-optical techniques, techniques in microwave and antenna measurement, and the time-domain solution of 3-D electromagnetic problems.

Linda Chen received the A.B. degree in mathematics (with honors) from Harvard University, Cambridge, MA, in 1996, and is currently a graduate student in mathematics at the University of Chicago, Chicago, IL.

During the summers of 1995 and 1996, she worked in the Submillimeter Receiver Laboratory of the Smithsonian Astrophysical Observatory, Cambridge, MA. Her current research interests include algebraic geometry and geometric invariant theory.

Raymond Blundell (M'91) was born in Liverpool, U.K. He received the B.Sc. and Ph.D. degrees in electrical and electronic engineering from the University of Leeds, Leeds, U.K.

In 1977, he joined the Thorn-EMI Group and was engaged in the development of scale-model radar systems. From 1980 to 1989, he was with the Institut of Radio Astronomie Millimétrique, Grenoble, France, leading a small group responsible for the development of low-noise millimeter heterodyne receivers. In 1989 he was made Director of the Sub-Millimeter Receiver Laboratory at the Harvard–Smithsonian Center for Astrophysics, Cambridge, MA, as well as being a Lecturer in astrophysics in the Department of Astronomy, Harvard University, Cambridge, MA. His research interests include millimeter and submillimeter techniques, superconducting tunnel-junction mixers, solid-state oscillators and frequency multipliers, low-noise amplifiers, quasi-optical components, and 4-K refrigeration systems.